Reaction of Gas-Phase Bromine Atom with Chemisorbed Hydrogen Atoms on a Silicon(100)-(2×1) Surface

Jongbaik Ree,[*] Kyung Soon Chang,[†] Kyeong Hwan Moon,[†] and Yoo Hang Kim[‡]

Department of Chemistry Education, Chonnam National University, Kwangju 500-757, Korea
[†]Department of Chemistry, Chonnam National University, Kwangju 500-757, Korea
[‡]Department of Chemistry and Center for Chemical Dynamics, Inha University, Inchon 402-751, Korea
Received May 2, 2001

The reaction of gas-phase atomic bromine with highly covered chemisorbed hydrogen atoms on a silicon surface is studied by use of the classical trajectory approach. It is found that the major reaction is the formation of HBr(g), and it proceeds through two modes, that is, direct Eley-Rideal and hot-atom mechanism. The HBr formation reaction takes place on a picosecond time scale with most of the reaction exothermicity depositing in the product vibration and translation. The adsorption of Br(g) on the surface is the second most efficient reaction pathway. The total reaction cross sections are 2.53 Å^2 for the HBr formation and 2.32 Å^2 for the adsorption of Br(g) at gas temperature 1500 K and surface temperature 300 K.

Keywords : Bromine, Hydrogen, Silicon, Eley-Rideal, Hot-atom.

Introduction

In gas-adatom interaction taking place on a solid surface, important reactive events involve the dissociation of the adatom-surface bond and association of the gas atom with the desorbing adatom. Such interactions are often highly exothermic, so there is a large amount of energy to be deposited in the various motions of the product. For example, chemisorption energies of atoms such as hydrogen and chlorine on a close-packed metal surface lie in the range of 2-3 eV,[1,2] whereas the energy of the bond formed between such atoms is 4-5 eV.[3] Thus, the reaction exothermicity is about 2 eV, which is to be distributed among various motions of the product, including the solid phase. So far, most studies have been performed on these type of reaction, that is, the highly exothermic reactions. The exothermicity is still very significant in the reactions involving a nonmetallic surface such as graphite and silicon as well.[4-8] Recently, we have studied the reaction of gas-phase chlorine or hydrogen atom with highly covered chemisorbed hydrogen atoms on a silicon surface, and reported that the mechanism of the reactions is the Eley-Rideal type.[9] In fact, an Eley-Rideal (ER) mechanism has been proposed to study such exothermic gas-surface reactions, most involving chemisorbed hydrogen atoms.[10-17]

However, if the gas-phase atom is bromine, even though it belongs to the same halogen group as chlorine, it doesn't lead to a highly exothermic reaction but to a slightly endothermic reaction. Thus, in the case of bromine we can expect the reaction mechanism to be quite different from the highly exothermic chlorine or hydrogen reactions. Furthermore, in such reactions where the surface is covered either sparsely or completely by chemisorbed hydrogen atoms, the possible reaction pathways depend on the surface coverage of the solid surface. Therefore, it should be interesting to study the reaction mechanism of gas-phase bromine atom reacting with chemisorbed hydrogen atoms on a silicon surface, in which the exothermicity is slightly endothermic (ΔE = 0.008 eV).

In the present paper, we have studied the reaction of gas-phase bromine atom with a H-saturated silicon surface. Especially, we have addressed what the reaction mechanism of gas-phase atomic bromine with chemisorbed hydrogen atoms on silicon(001)-(2×1) surface is in the case of high surface coverage. In this model, one hydrogen atom is adsorbed on each silicon atom on the surface. That is, the adsorbed hydrogen atoms form a monolayer and the surface silicon atoms form monohydrides. The monohydrogenated case has been shown to be of major improtance over the dihydrogenated or trihydrogenated cases.[4,18] To study the reaction, we have followed the time evolution of the pertinent coordinates and conjugate momenta of each reactive trajectory on a London-Eyring-Polanyi-Sato (LEPS) potential energy surface, which is constructed with many-body interactions operating between all atoms of the reaction system. The time evolution of the trajectories was determined by solving the equations of motion formulated by uniting gas-surface procedure and generalized Langevin theory for the solid phase.[19,20]

Interaction Model

The interaction model and the numerical procedures have already been reported in detail in Ref. 9. The interaction model is the same as the one in Ref. 9 except that the chlorine atom is now replaced by the bromine atom. We summarize the essential aspects of the interaction and the numerical procedures on the silicon (001)-(2×1) surface reconstructed by forming dimers along the [110] direction

[*]Author to whom correspondence should be addressed. e-mail: jbree@chonnam.ac.kr

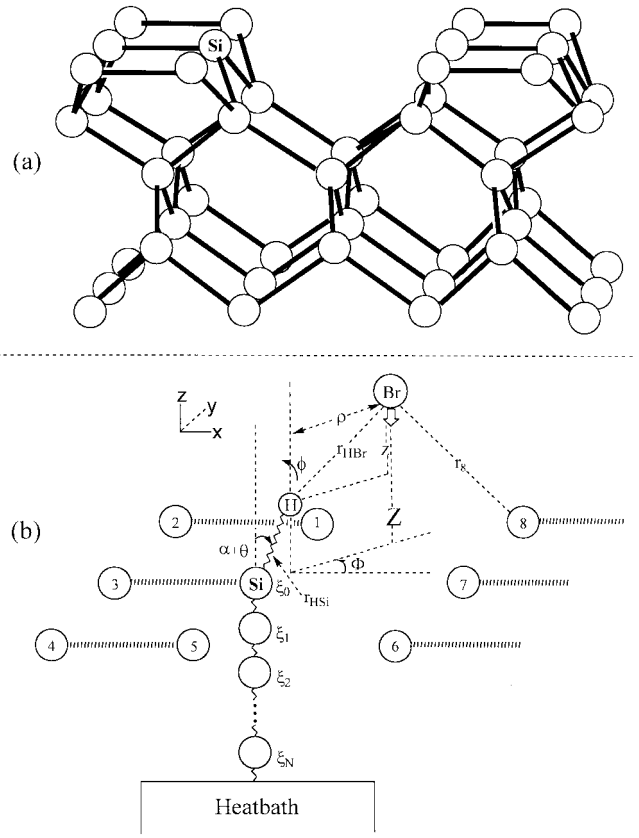

Figure 1. (a) Symmetric Si-Si dimer surface. (b) Interaction model showing the H atom adsorbed on the *0*th Si atom, which is coupled to the *N*-atom chain. The coordinates of the (*N*+1) chain atoms including the 0th atom are denoted by 0, 1, ..., *N*. The *0*th atom is identified by Si in both (a) and (b). The *N*th atom of the chain is coupled to the heat bath. The position of H is defined by (r_{HSi},θ,ϕ) and the position of Br by (ρ,Z,Φ). α is the tilt angle. The Br to H distance is denoted by r_{HBr}, and the Br to the *i*th surface-layer Si atom distance by r_i.

[Figure 1(a)]. For easy reference we have displayed the collision model in Figure 1(b). The H atom is chemisorbed on the Si atom of the symmetric dimer structure. This Si atom is the zeroth member of the (*N* + 1)-atom chain which links the reaction zone to the heat bath. Furthermore, the zeroth Si atom is surrounded by eight nearby Si atoms identified by numbers 1, 2, ..., 8 in Figure 1(b). The reaction zone atoms are the zeroth Si atom, the adatom, and the incident Br gas atom. We condsider that these reaction zone atoms, eight surrounding Si atoms, and the *N*-chain atoms constitute the primary system. We then designate the remaining infinite number of solid atoms as secondary atoms.

A total of six degrees of freedom is necessary to describe the motions of Br and H atoms above the surface. Although it is straightforward to transform these coordinates to the center-of-mass and relative coordinate systems, we find it convenient to describe the collision system including surface atoms in terms of the atomic coordinates $H(x_H,y_H,z_H)$ and $Br(x_{Br},y_{Br},z_{Br})$. The H coordinates are $x_H = r_{HSi}\sin(\alpha + \theta)\cos\phi$, $y_H = r_{HSi}\sin(\alpha + \theta)\sin\phi$, and $z_H = r_{HSi}\cos(\alpha + \theta)$, *i.e.*, $H(x_H,y_H,z_H) = H(r_{HSi},\theta,\phi)$. Prior to desorption, the adatom tilted at an angle of $\alpha = 20.6^{o}$ [21] undergoes hindered motions along θ and ϕ. For the position of Br with respect to the surface normal axis through the adatom, we define two coordinates ρ and z such that the Br-H interatomic distance r_{HBr} is $(\rho^2 + z^2)^{1/2}$, where ρ is the perpendicular distance between Br and the H-surface normal axis, and z is the vertical distance from Br to the horizontal line determining the position of H. Note that the initial ($t \to -\infty$) value of ρ is the impact parameter *b*. The projection of r_{HBr} on the surface plane is oriented by the angle Φ from the *x* axis. Thus, the coordinate (x_{Br},y_{Br},z_{Br}) can be transformed into the cylindrical system (ρ,Z,Φ), where *Z* is the Br-to-surface distance. The vertical distance *z* is then $z = Z - r_{HSi}\cos(\alpha + \theta)$. The occurrence of each reactive event can be determined by studying the time evolution of the Br-surface distance *Z*, the H-Si bond distance r_{HSi}, and the Br-to-H distance $r_{HBr} = (\rho^2 + z^2)^{1/2}$ for the ensemble of gas atoms approaching the surface from all directions. The initial state is chosen to be that of the gas atom approaching the surface with the collision energy *E*, impact parameter *b*, and azimuthal angle Φ from a large distance from the surface ($\approx$20 Å), where the adatom is in the initial set of (r_{HSi},θ,ϕ).

A convenient expression of the interaction potential can be obtained in a modified form of the London-Eyring-Polanyi-Sato (LEPS) potential energy surface for the interactions of Br to H, H to Si, and Br to nine surface-layer Si atoms including the θ- and ϕ-hindered rotational motions and the harmonic motions of the (*N* + 1)-chain atoms to obtain the overall interaction energy:

$$\begin{aligned} U = \{&Q_{HBr} + Q_{HSi} + Q_{BrSi} - [A_{HBr}^2 + A_{HSi}^2 + A_{BrSi}^2 \\ &- A_{HBr}A_{HSi} - (A_{HBr} + A_{HSi})A_{BrSi}]^{1/2}\} \\ &+ 1/2k_\theta(\theta - \theta_e)^2 + 1/2k_\phi(\phi - \phi_e)^2 + \sum_j (1/2M_s\omega_{ej}^2\xi_j^2) \\ &+ \sum_j (\text{terms of type } M_s\omega_{cj}^2\xi_{j-1}\xi_j,\ M_s\omega_{c,j+1}^2\xi_j\xi_{j+1}, \text{ etc}), \end{aligned} \quad (1)$$

where k_θ and k_ϕ are force constants, θ_e and ϕ_e are the equilibrium angles, M_s is the mass of the silicon atom, ω_{ej} is the Einstein frequency, and ω_{cj} is the coupling frequency characterizing the chain. The explicit forms of the coulomb terms (*Q*'s) and exchange terms (*A*'s) for HBr, HSi, and BrSi are given in Ref. 22. In Eq. (1), Q_{BrSi} and A_{BrSi} each contains nine terms for the Br-Si_0, Br-Si_1, ..., Br-Si_8 interactions. Since $r_i \equiv r_i(r_{HSi}, \theta, \phi, \rho, Z,)$ and $r_{HBr} \equiv r_{HBr}(r_{HSi}, \theta, \rho, Z)$, the potential energy surface has the functional dependence of $U(r_{HSi},\theta,\phi,\rho,Z,\Phi,\{\xi\})$, where $\{\xi\} = (\xi_0,\xi_1,...,\xi_N)$ for the vibrational coordinates of the (*N* + 1)-chain atoms.

The potential and spectroscopic constants for the H$\cdots$Br interaction are[23] $D_{HBr} = D^0_{0,HBr} + 1/2\hbar\omega_{HBr} = 3.622$ eV, $D^0_{0,HBr} = 3.458$ eV, $a_{HBr} = (D_{HBr}/2\mu_{HBr})^{1/2}/\omega_{HBr} = 0.265$ Å, $\omega_{HBr}/(2\pi c) = 2649$ cm^{-1}, and $\mu_{HBr} = m_H \times m_{Br}/(m_H + m_{Br})$. For the H-Si bond, potential and spectroscopic constants are $D_{HSi} = D^0_{0,HSi} + 1/2\hbar\omega_{HSi} = 3.630$ eV, $D^0_{0,HSi} = 3.50$ eV,[24,25] $a_{HSi} = (D_{HSi}/2\mu_{HSi})^{1/2}/\omega_{HSi} = 0.334$ Å, $\omega_{HSi}/(2\pi c)$=2093 cm^{-1}.[5,26] Here μ_{HSi} is the reduced mass associated with the H-Si bond. The planar *x*- and *y*-direction vibrational frequencies on the surface are known to be 645 cm^{-1}.[5] The equilibrium distances of the H-Br and H-Si bonds are 1.414[23] and 1.514

Å,[26] respectively. For the Br-surface interaction, we take D_{BrSi} = 0.245 eV,[27] a_{BrSi} = 0.35.[22] We also take the equilibrium separation of the Br-surface as 4.0 Å.[28]

For this reaction, the activation energy is known to be only ~1.0 kcal/mole.[29,30] After systematically varying the values of the Sato parameter Δ's, we find that the set Δ_{HBr} = 0.30, Δ_{HSi} = 0.63 and Δ_{BrSi} = 0.37 for the Br to the surface Si atoms, describe best the desired features, minimizing the barrier height and the attractive well in the product channel.

Once the potential energy surface (PES) is determined, we can follow the time evolution of the primary system by integrating the equations of motion, which describe the motions of the reaction-zone atoms and *N*-chain atoms. We expect that this PES will enable us to understand how gas atoms and adsorbate atoms react with each other and then desorb from the surface. An intuitive way to treat the dynamics of the reaction involving many surface atoms is to solve a united set of equations of motion for the reaction-zone atoms and the Langevin equation for *N*-chain atoms, which couples the reaction zone to the heat bath. The gas-adatom part of the resulting equations are $m_i \ddot{Y}_i(t) = -\partial U/\partial Y_i$, where $Y_1 = Z$, $Y_2 = \rho$, $Y_3 = \Phi$, $Y_4 = r_{HSi}$, $Y_5 = \theta$, $Y_6 = \phi$, with $m_1 = m_{Br}$, $m_2 = \mu_{HBr}$, $m_3 = I_{HBr}$, $m_4 = \mu_{HSi}$, $m_5 = m_6 = I_{HSi}$. Here μ_i and I_i are the reduced mass and the moment of inertia of the interaction system indicated. For the $(N + 1)$-atom chain, which includes the zeroth Si atom, the equations are

$$M_s \ddot{\xi}_0(t) = -M_s \omega_{e0}^2 \xi_0(t) + M_s \omega_{c1}^2 \xi_1(t) - \partial U(z_{HSi}, \theta, \phi, \rho, Z, \Phi, \{\xi\})/\partial \xi_0 \quad (2a)$$

$$M_s \ddot{\xi}_j(t) = -M_s \omega_{ej}^2 \xi_j(t) + M_s \omega_{cj}^2 \xi_{j-1}(t) + M_s \omega_{c,j+1}^2 \xi_{j+1}(t), \quad j = 1, 2, .., N-1 \quad (2b)$$

$$M_s \ddot{\xi}_N(t) = -M_s \Omega_N^2 \xi_N(t) + M_s \omega_{c,N}^2 \xi_{N-1}(t) - M_s \beta_{N+1} \dot{\xi}_N(t) + M_s f_{N+1}(t) \quad (2c)$$

Equation (2a) is for the vibration of the zeroth chain atom on which the H atom is chemisorbed. Equation (2c) is for the vibration of the *N*th atom which is bound to the bulk phase. The *N*th Si is directly linked to the heat bath, and through this coupling the heat bath exerts systematic dissipative and random (or stochastic) forces on the primary system composed of the reaction zone atoms and the *N*-chain atoms. Ω_N is the adiabatic frequency. The friction coefficient β_{N+1} is very close to $\pi\omega_D/6$, where ω_D is the Debye frequency, and governs the dissipation of energy from the primary zone to the heat bath. All values of β, ω_e, ω_c, and Ω are presented elsewhere.[31] The quantity $M_s f_{N+1}(t)$ is the random force on the primary system arising from thermal fluctuation in the heat bath. This force balances, on average, the dissipative force, $M_s\beta_{N+1}(t)$, which removes energy from the $(N + 1)$ atom chain system in order that the equilibrium distribution of energies in the chain can be restored after collision.

The computational procedures make use of Monte Carlo routines to generate random numbers for the initial conditions. The first of them is the collision energies *E* sampled from a Maxwell distribution at the gas temperature T_g. In sampling impact parameters *b*, we note that the distance between the hydrogen atoms adsorbed on the nearest Si sites is 3.59 Å. Thus, we take the half-way distance so that the flat sampling range is $0 \leq b \leq 1.80$ (*i.e.*, b_{max} = 1.80 Å). In the collision with $b > 1.80$ Å, the gas atom is now in the interaction range of the hydrogen atom adsorbed on the adjacent surface site. The initial conditions and numerical techniques needed in solving the equations of motions are given in detail elsewhere.[22,32] To ascertain what really happens during the reaction, we followed each trajectory for sufficiently long time, 50ps.

Results and Discussion

Reaction probabilities. Since the typical experimental condition for producing bromine atoms is 1500 K,[33] we considered the reaction occurring at the gas temperature of 1500 K. At the thermal conditions of (T_g,T_s) = (1500, 300 K), we find that mainly the following two reactions occur:

$$Br(g) + H(ad)/Si \rightarrow HBr(g) + Si, \quad P_{(i)} = 0.200 \quad (i)$$

$$Br(g) + H(ad)/Si \rightarrow Br(ad)/Si + H(ad)/Si, \quad P_{(ii)} = 0.122 \quad (ii)$$

The reaction probability $P_{(j)}$ for reaction (*j*) at the gas and the surface temperature (T_g,T_s) is defined as the ratio of the number of respective reactive trajectories N_R to the total number of trajectories N_T (60,000) sampled over the entire range of impact parameters. Reaction (i) is the most important reactive event. This event leads to HBr formation, the reaction probability being $P_{(i)}$ = 0.200. For a rather small fraction of the trajectories, the incident bromine atom is trapped without dissociating the surface H-Si bond. In the present calculation, the exchange reaction, Br(g) + H(ad)/Si → Br(ad)/Si + H(g), was not found. These results are similar with those for Cl(g) interacting with H(ad)/Si[9] or H(D)(g) interacting with D(H)/Si,[5,6,34] in that the primary reaction pathway is the gas phase molecule, *i.e.*, HCl(g) or HD(g), formation. Especially, HBr formation probability is very close to the HCl formation probability (*P* = 0.175). Despite the fact that HBr formation reaction is slightly endothermic, the probability for endothermic HBr formation is quite large. The energy to overcome the endothermicity (0.008 eV) comes mainly from the ensemble-averaged kinetic energy of the incident Br atom (E_{kin} = 0.194 eV) and the zero-point energy of Si-H vibration (E_{vib} = 0.130 eV). Also this probability is as large as that for exothermic HCl formation. This is because Br atom is heavier than Cl atom so that Br atom can pick up H atom more easily. The same effect can be seen when one compares H + H/Si and Cl + H/Si systems. Even though the exothermicity of the reaction is about the same for both systems (0.978 eV and 0.934 eV, respectively), the probability for HCl formation (*P* = 0.175) is larger than that for H_2 formation (*P* = 0.076) because Cl is much heavier than H.[9,32]

It should be also interesting to note that, in their calculation for hydrogen abstraction from copper surface, *i.e.*, D(H) + H(D)/Cu(111) system,[35] Rettner and Auerbach reported that HD formation and trapping probabilities are almost the same (~0.47) with a small fraction scattering at

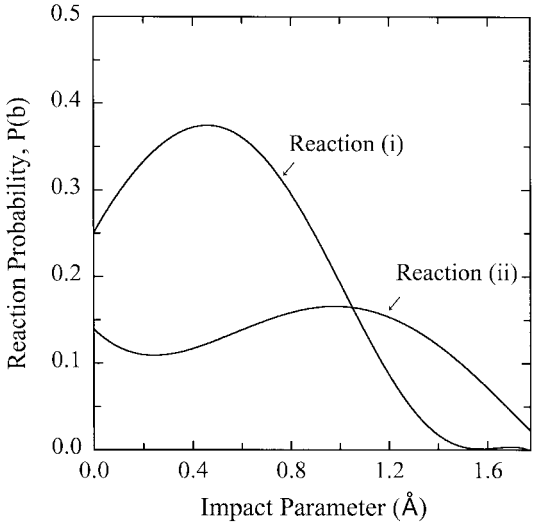

Figure 2. Dependence of the opacity function $P_{(i)}(b)$ on the impact parameter for reactions (i), HBr formation; and (ii), Br adsorption.

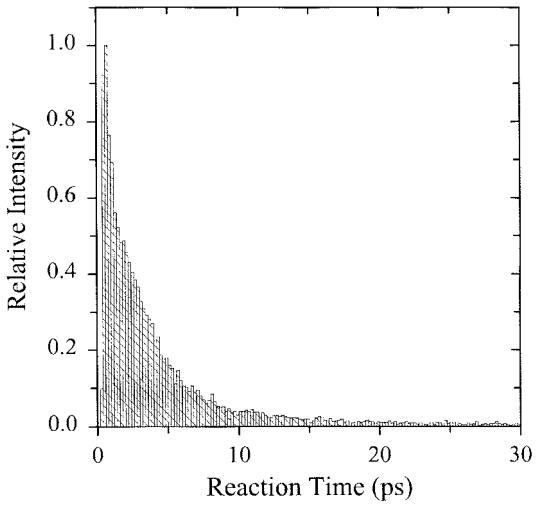

Figure 3. Reaction time distribution for reaction (i), HBr formation.

the point of impact. They also noted that no exchange process could be detected for a 0.07 eV H-atom beam with $\theta_i = 10^o$ with a D-saturated surface. As mentioned earlier, no exchange process was found in our system, either.

The probability $P_{(j)}$ defined above is the total probability at the specified thermal conditions of T_g and T_s. However, it is also important to analyze the dependence of the extent of reaction on the impact parameter. We plot the b dependence of the opacity function $P_{(j)}(b)$ for the primary reaction pathways (i) and (ii) in Figure 2. As shown in Figure 2, $P_{(i)}(b)$ is 0.25 in $b \cong 0$ collisions and then rises to a maximum value near $b = 0.5$ Å and then decreases to zero with increasing b. This indicates that the reaction (i) occurs mostly in the neighborhood of the adatom site. Generally, the same trend was found in Cl+H/Si system too. In their quasi-classical study of Eley-Rideal recombinative desorption of H_2 from Cu(111), Persson and Jackson[36] also found that the dominant contribution to the cross section comes from a narrow range of impact parameters. From the b-dependent reaction probability we can calculate the total reaction cross section of 2.53 Å^2 for the reaction (i) from the expression: $\sigma = 2\pi\int_0^{b_{max}} P(T_g, T_s;b)b\, db$. This reaction cross section is larger than that of the related system Cl(g) + H(ad)/Si (*i.e.*, 1.19 Å^2).[9] The reason why the reaction cross section for Br+H/Si system is larger than that for Cl+H/Si is that $P(b)$ values for the former are generally higher than that for the latter. On the other hand, the opacity function $P_{(ii)}(b)$ for the reaction (ii) is smaller than that of the reaction (i) over the small b range, but it is larger in the large b ($b \geq 1.1$ Å) range. The total cross-section for the trapping reaction (ii) is 2.32 Å^2. These findings are quite different from those of Persson and Jackson for the Eley-Rideal recombinative desorption of hydrogen on Cu(111) surface. According to their flat surface model calculation, the cross-sections for direct Eley-Rideal recombination forming H_2(g), for non-reactive exchange scattering and for the trapping of incident H atom are 0.5, 0.003 and 20 Å^2, respectively.[36] This is because in our model the surface is fully covered with H atoms, while in Persson and Jackson's model the Cu surface is only sparsely covered. We now discuss the details of each of these reaction pathways, with a greater emphasis on the HBr formation, reaction (i).

Reaction (i). Figure 3 shows the distribution of reaction times for the HBr formation reaction (i). To determine this time scale, we first confirm the occurrence of a reactive event by following the motion of HBr(g) for 50 ps. When HBr(g) does not adsorb on the surface and is completely away from the influence of surface interactions, we trace the reactive trajectory backward to find the time at which the H to Si separation has reached $r_{HSi,e}$ + 5.0 Å,[7] where $r_{HSi,e}$ is the equilibrium distance of the H-Si bond (1.514 Å). We define the period from the start of collision to the time at which the H-Si distance reaches ($r_{HSi,e}$ + 5.0) Å as the reaction time t_R for the reaction (i). (We will consider this reaction time in detail in the discussion of Figure 4.)

As shown in Figure 3, almost all type (i) events (10,756 out of 11,978) were completed within 10 ps. The ensemble-averaged reaction time is 4.11 ps. Peden et al. suggested that the reactions which are completed within 10 ps follow the Eley-Rideal mechanism.[37] According to this suggestion, the HBr formation (reaction (i)) can be considered as Eley-Rideal type reaction in a broad sense. However, an important question still remains to be answered. The question is whether these reactive events occur during single impact or multiple impact collisions. To find out what really happens during the gas-surface collisions, we examined each reactive trajectory in more detail. About one fourth of the total 11,978 reactive trajectories leading to reaction (i) occur on a subpicosecond time scale (see Figure 3), during which the adatom suffers only one impact with the surface. In such a direct-mode collision, the incident atom accelerates before and after impact. When the incident atom turns around, it can pick up the adatom that is oscillating between the two heavy atoms Br and Si. These events may be regarded as Eley-Rideal type reaction in the strictest sense.

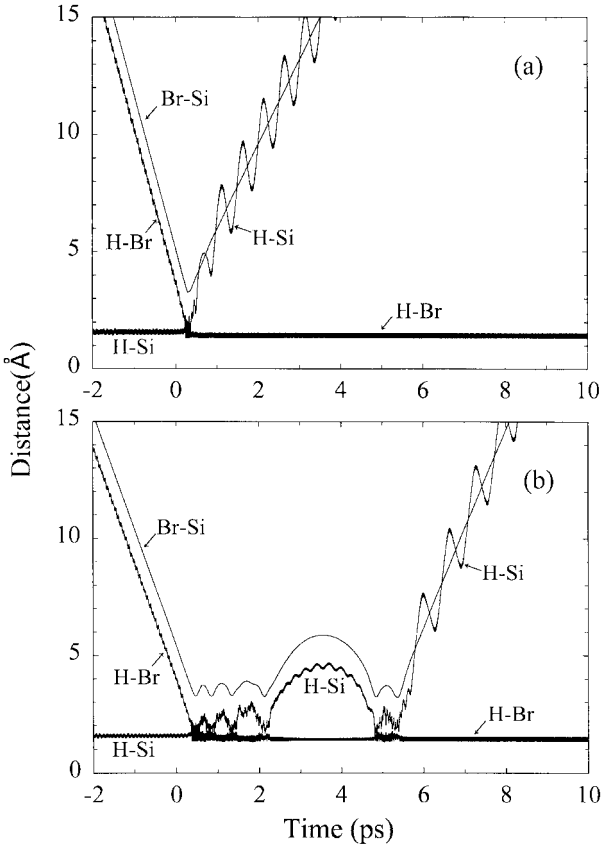

Figure 4. Dynamics of the representative trajectory for (a) a direct-mode collision, (b) a hot-atom collision in reaction (i). The time evolution of the Br to surface, HSi, and HBr distances.

In order to study the direct mode reaction dynamics in detail, we select a trajectory which is representative of direct-mode collisions of reaction (i) and plot the time evolution of its gas atom-surface distance Z (*i.e.*, the collision trajectory), adatom-surface distance r_{HSi}, and the Br to H distance r_{HBr} in Figure 4(a). The reaction time of this representative case is 0.75 ps. Rigorously speaking, the outgoing portion of Z is not the trajectory. However, since $m_{Br} >> m_H$, the center of mass HBr is very close to Br and therefore Z can be considered as the outgoing trajectory. The oscillation of the outgoing r_{HSi} is due to the rotation of HBr. It is not possible to determine when the reaction begins from the time evolution of Z shown in Figure 4(a). However, near $t = 0$, when Br to surface distance is 6 Å, the H to Br interaction energy begins to decrease, indicating the start of reaction. As shown in Figure 4(a), the Br atom reaches the turning point at $t = 0.20$ ps, and then the product HBr recedes to 5 Å from the surface at $t = +0.75$ ps. Thus, we can say that the collision begins (or ends) when the incident atom (or product molecule) reaches a distance of 5-6 Å from the surface. Our choices of 5.0 Å for H-Si displacement as the occurrence of a reactive event and the above-defined reaction time scale are based on this time evolution. The number of trajectories by this direct Eley-Rideal mechanism is 3,164 out of the total 11,978 reactive trajectories following reaction (i).

There are remaining 8,814 reactive events in which multiple impacts occur. These events may be considered as hot-atom mechanism. A typical case of them is shown in Figure 4(b). As shown in Figure 4(b), the Br-to-surface interaction begins near $t = 0$, and the incident Br atom suffers the first impact with the surface near $t = +0.5$ ps. At this time, the Br atom comes in close range of the adatom causing a significant disturbance in the H-Si interaction. Unlike the single impact collision in Figure 4(a), the Br atom does not pick up the adsorbed H atom and fly away with it. In this case, the Br atom stays on the surface for a long time and experiences multiple impact collision. As shown in Figure 4(b), the trapped Br atom rebounds several times, spending a relatively long time above the surface. This is a barely trapped trajectory, thus forming a loosely bound complex on the surface, Br-H-Si. A fine structure in the H-Br distance during the large amplitude oscillation is due to the H-Br vibration. After completing several oscillations, the Br atom is attracted back to the surface for final impact near $t = +5.4$ ps, at which time Br abstracts H and turns the corner to move away from the surface. The receding molecule reaches a distance of 6 Å at $t = +5.8$ps. This reaction time is not long enough to invoke a LH mechanism, in which reactions are believed to occur between chemisorbed species that are in thermal equilibrium with the surface, and we regard this event to follow a hot-atom mechanism. In a classical trajectory study of H(D) + D(H)/Si(100) system, Kratzer also found that more than half of HD formation was due to the multiple impact (hot atom) collisions.[25]

We now consider the distribution of ensemble-averaged energies in the product state. The vibrational population distribution of HBr produced in reaction (i) is shown in Figure 5(a). The population is a typical Boltzmann distribution with the maximum between 0 and 0.1 eV. A clearer presentation is Figure 5(b), where the intensity mimics the quantum vibrational distribution formulated by use of a binning procedure of assigning quantum number v_{HBr} corresponding to $v_{HBr} = \text{int}[E_{vib}/E_{vib}(v_{HBr})]$. Here E_{vib} is the vibrational energy calculated in the present study and $E_{vib}(v_{HBr})$ is the vibrational energy determined from the eigenvalue expression $E_{vib}(v_{HBr})/hc = \omega_e(v_{HBr} + 1/2) - \omega_e x_e(v_{HBr}+1/2)^2 + \omega_e y_e(v_{HBr}+1/2)^3$ with $\omega_e = 2648.98$ cm^{-1}, $\omega_e x_e = 45.217$ cm^{-1}, $\omega_e y_e = -0.003$ cm^{-1}. As shown in Figure 5(b), the binning procedure yields the intensities of 0.971, 0.028, and 1.62×10^{-4} for $v_{HBr} = 0$, 1, and 2, respectively. These values are close to the Boltzmann distribution at 1000 K, that is, the intermediate temperature between gas (1500 K) and surface temperature (300 K), which predicts the fractions 0.978, 0.022, and 4.74×10^{-4} for $v_{HBr} = 0$, 1, and 2, respectively.

In reaction (i) the rotational energy is calculated as $E_{rot} = L^2/2\mu_{HBr}r_{HBr}^2$, where the angular momentum $L = \mu_{HBr}(z\dot{\rho} - \rho\dot{z})$ with the corresponding quantum number $J = L/\hbar$. As in the above-discussed vibrational quantum number, the rotational quantum number J_{HBr} corresponding to the rotational energy E_{rot} can be calculated through the relation $J_{HBr} = \text{int}[E_{rot}/E_{rot}(J_{HBr})]$, where $E_{rot}(J_{HBr}) = J_{HBr}(J_{HBr} + 1)\hbar^2/2I_{HBr}$. The maximum occurs at $J_{max} = 2$[see Figure 6(a)]. If we take

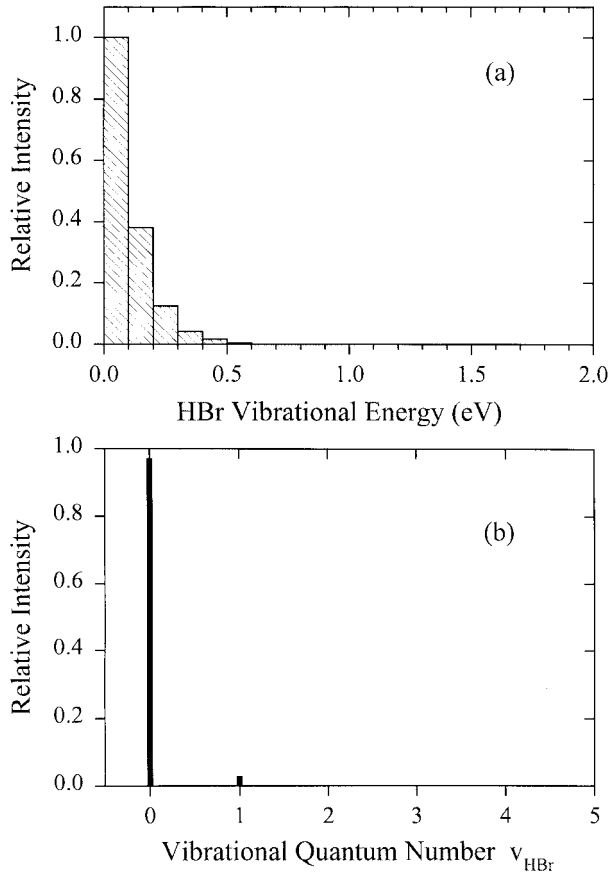

Figure 5. Vibrational population distribution of HBr in reaction (i). (a) Relative intensity *vs.* the HBr vibrational energy. (b) Intensity *vs.* the vibrational quantum number.

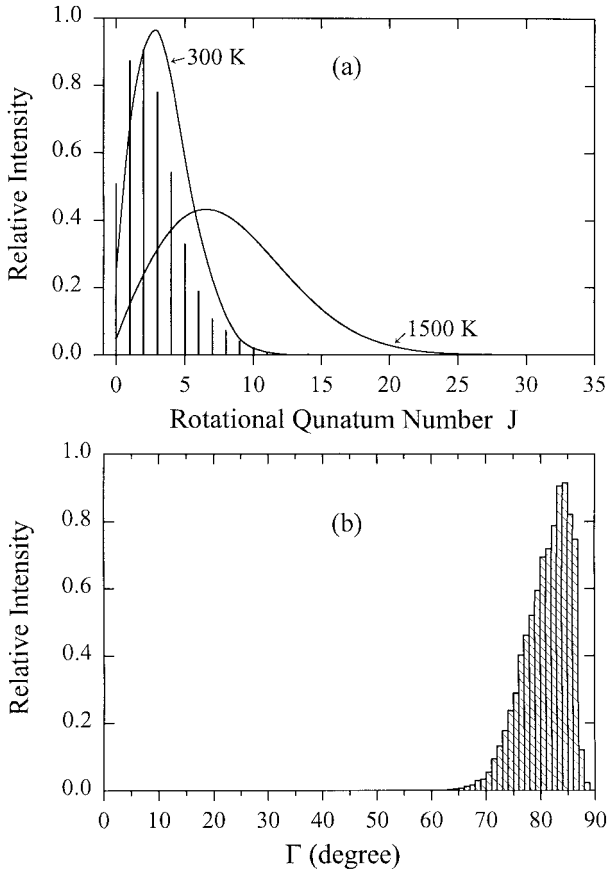

Figure 6. (a) Relative intensity of the rotational population distribution of HBr in reaction (i). (b) Distribution of the angle between the axis of HBr rotation and the surface normal Γ for reaction (i).

the gas temperature of 1500 K, the rotational maximum obtained from the Boltzmann expression $J_{max} = 1/2[(2\ kT/\bar{B})^{1/2}–1]$ with $\bar{B} = 10.34\ cm^{-1}$ is 7. On the other hand, for the surface temperature of 300 K, the Boltzmann intensity is sharply peaked at $J_{max} = 3$. The shape and intensity distribution of the present calculation shows that the rotational motion of product HBr is close to the Boltzmann distribution at $T_g = 300$ K. In addition to this rotational population distribution, it is interesting to know how the desorbing HBr molecules are rotationally aligned at the instant of desorption. To examine this aspect, we have calculated the angle between the axis of rotation of HBr and the surface normal when the Br atom turns the corner after the final impact and begins the journey outward with H. The angular distribution is found to be sharply peaked near 90°, indicating that the rotational axis is closely parallel to the surface [see Figure 6(b)]. That is, the product molecules leave the surface in a cartwheel-like rotation.

The ensemble-averaged translational energy of HBr produced in reaction (i) is as large as 0.091 eV, and we now look into the velocity distribution of these molecules. Figure 7 shows a time-of-flight distribution of HBr product molecules along with the fitted curve. The points are obtained by collecting molecules reaching the "reaction chamber-to-detector" distance of 30 cm. As shown in Figure 7, the HBr

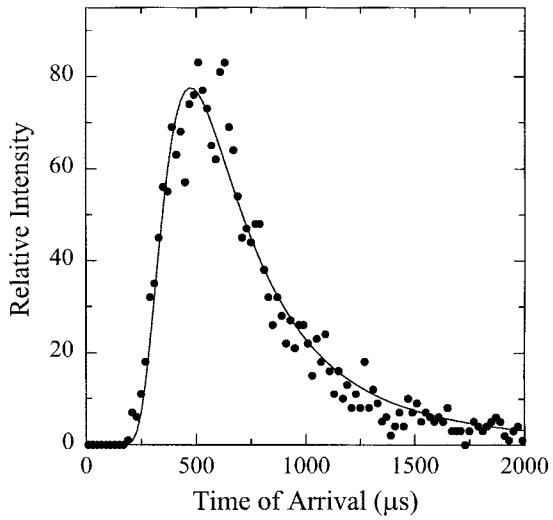

Figure 7. Time-of-flight distribution for HBr in the reaction (i) from the surface.

molecules reach the detector much later than the HCl from the related system Cl(g) + H(ad)/Si for which the maximum intensity occurs at 200 μs. It is because Br atom is much heavier than Cl atom and also the translational energy of the

desorbing HBr molecule is smaller than that of HCl. Although there is a significant number of slowly moving molecules near and above 1300 μs, the distribution of most points fits well with a velocity function of the form $f(v) = Av^3 e^{-(v-v_0)^2/\alpha^2}$ with $A = 9.33 \times 10^{-7}$, $v_0 = 163$ m/s and $\alpha = 445$ m/s. The velocity distribution takes the maximum value at $v_{max} = 1/2[v_0 + (v_0^2 + 6\alpha^2)^{1/2}] = 633$ m/s, which gives $1/2m_{HBr}v_{max}^2 = 0.168$ eV. This energy is comparable to $3/2kT_g = 0.194$ eV, indicating that the velocity of the fast moving molecules closely follows the Boltzmann distribution at $T_g = 1500$ K. We note that this energy is in far excess of $kT_s = 0.026$ eV. Figure 7 also shows a significant number of product molecules reaching the detector at a time longer than 1300 μs. These slowly moving molecules are associated with reaction times of several picoseconds. These collisions represent a distinctly different class of gas-surface reactions compared to the short-time events (or direct collisions) for the present reaction. For these collisions it is reasonable to assume that the Br atoms are first adsorbed and then proceed to react with H atoms on the surface. They are trapping-mediated reactions, occurring in an indirect or hot-atom collision. Thus, they have had a quite sufficient time to accomodate, at least partially, to the surface, and then leave the surface with a temperature close to T_s. From the above-mentioned results one can calculate the fractions of available energy deposited to various modes of product HBr molecule. The ensemble averaged fractions are 0.46, 0.44 and 0.09 for vibrational, translational and rorational motion, respectively.

The ensemble-averaged energy transfer to the silicon surface $<E_s>$ is –0.027 eV, which means the desorbing HBr molecule takes away energy from the surface. In other systems such as H+H/Si and Cl+H/Si, the $<E_s>$ values were approximately +0.1 eV,[9,32] which means that the solid surface gain energy after collision. In Br+H/Si system, however, $<E_s>$ is negative reflecting the fact that the system must gain energy from the surface for the endothermic reaction to occur.

Reaction (ii). The reaction probability $P_{(ii)}$ calculated at (1500, 300 K) is only 0.122. In this case, the Br atom interacts with the adatom to form a weak H-Br bond and the interaction is not strong enough to break the H-Si bond. As shown in Figure 2, the distribution of impact parameters indicates that this reaction occur over all *b* collisions. For several representative trajectories of this reaction, we have followed the Br-surface distance for 50 ps but found no evidence of dissociation; the adsorbed Br becomes fully equilibrated on the surface [see Figure 8(a).] Furthermore, the time evolution of the Br-surface distance during such a long time with a well-organized low frequency oscillation indicates that the Br dissociation at some later time is highly unlikely. The desorption would be possible if the Br atom interacts with a large amount of collision energy, but such a collision would lead to reaction (i). The reaction (ii) is dominated by low-*E* collisions. The time evolution plotted in Figure 8(a) shows the H-Br distance undergoing a low-frequency oscillation corresponding to the stable Br-surface motion, because Br is bound to both H and the surface. The

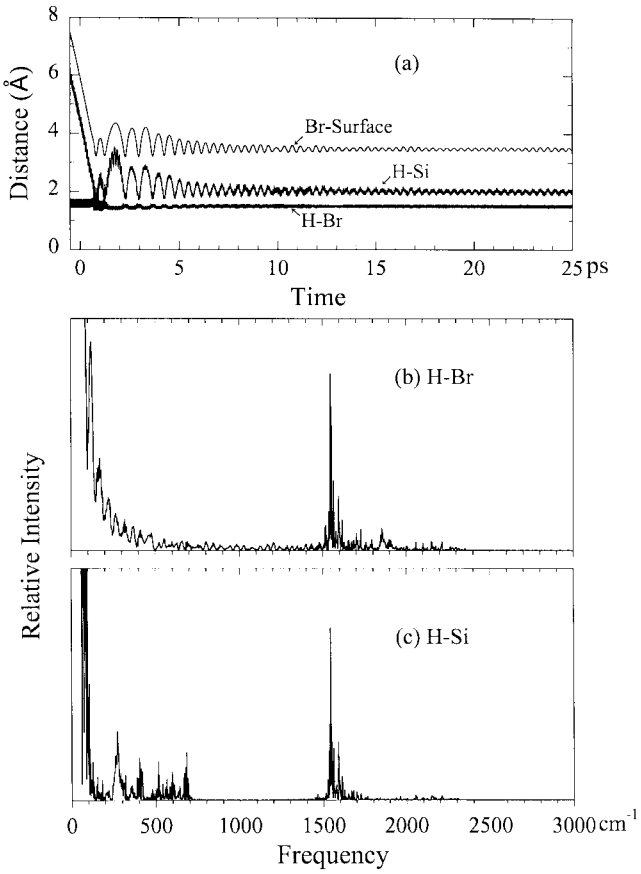

Figure 8. (a) Time evolution of the Br to surface, H-Br and H-Si distances for a representative collision in reaction (ii). (b) Power spectrum of the H-Br vibration. (c) Power spectrum of the H-Si vibration.

low-frequency oscillation of the Br-surface distance shown in Figure 8(a) also clearly indicates that the Br atom undergoes weak interaction with the surface. When Br approaches in close proximity of the surface, a repulsive force begins to act between Br and the surface atom, thus repelling Br. This repulsive energy and the attractive interaction generated by the preadsorbed atom coordinate to steer Br toward H. Thus, reaction (ii) can produce a three-atom configuration (Br-H-zeroth Si), where the Br-zeroth Si interaction is a physisorption type.

The power spectrum of the HBr vibration does not show a peak corresponding to the HBr fundamental vibrational frequency of 2649 cm^{-1} [see Figure 8(b)]. Instead, it shows peaks near 1500 cm^{-1}, which is the frequency of the highly excited stretching vibrational motion of adatom H. The peaks appearing below 100 cm^{-1} are for the large-amplitude oscillation shown in both the H-Si and Br-surface distances in Figure 8(a). In fact, the H-Si bond executes a well-organized vibration since H is still tightly bound to the surface. [See Figure 8(a).] The peaks near 1500 cm^{-1} shown in Figure 8(b) represent this vibration. We also find a clearer spectrum of the H-Si vibration near 1500 cm^{-1} in Figure 8(c). The structure of the spectrum is primarily due to the disruption of H-Si vibration caused by the nearby Br atom.

In Figure 8(c), there are some peaks around 500 cm^{-1}, which is the frequency of the hindered motion of adatom of H along the θ direction. Thus, reaction (ii) does not represent the formation of trapped H-Br on the surface.

Concluding Comments

We have studied the interaction of gas phase atomic bromine with a highly covered chemisorbed hydrogen atoms on a silicon surface with particular emphasis on the reaction mechanism. At gas temperature 1500 K and surface temperature 300 K, the principal reaction pathway is the desorption of the product HBr(g) from the surface. In case of HBr(g) formation, less than half of reactive events occur on a subpicosecond time scale through direct-mode collisions, while remaining reactive events occur on reaction time scale longer than one picosecond through hot-atom collisions, which may be regarded as precursor type mechanism. The adsorption of Br(g) atoms without dissociating the H-surface bonds is the second most efficient reaction pathway.

In HBr formation, most of the reaction energy deposits in the vibrational and translational motions of HBr. The product HBr molecule leaves the surface in a cartwheel-like rotation.

Acknowledgment. This work was supported by a Korea Research Foundation Grant (KRF-99-015-DP0173). Computational time was supported by Supercomputing Application Support Program of the KORDIC Supercomputing Center.

References

1. Shustorovich, E. *Surf. Sci. Rep.* **1986**, *6*, 1.
2. Christmann, K. *Surf. Sci. Rep.* **1988**, *9*, 1.
3. *CRC Handbook of Chemistry and Physics*, 64th Ed.; Weast, R. C., Ed.; CRC Press: 1983; pp F176-F181.
4. Koleske, D. D.; Gates, S. M.; Jackson, B. *J. Chem. Phys.* **1994**, *101*, 3301.
5. Kratzer, P. *J. Chem. Phys.* **1997**, *106*, 6752.
6. Buntin, S. A. *J. Chem. Phys.* **1998**, *108*, 1601.
7. Ree, J.; Shin, H. K. *J. Chem. Phys.* **1999**, *111*, 10261.
8. Kim, Y. H.; Ree, J.; Shin, H. K. *Chem. Phys. Lett.* **1999**, *314*, 1.
9. Kim, W. K.; Ree, J.; Shin, H. K. *J. Phys. Chem. A* **1999**, *103*, 411.
10. Hall, R. I.; Cadez, I.; Landau, M.; Pichou, F.; Schermann, C. *Phys. Rev. Lett.* **1988**, *60*, 337.
11. Eenshuistra, P. J.; Bonnie, J. H. M.; Lois, J.; Hopman, H. *Phys. Rev. Lett.* **1988**, *60*, 341.
12. Kratzer, P.; Brenig, W. *Surf. Sci.* **1991**, *254*, 275.
13. Jackson, B.; Persson, M. *Surf. Sci.* **1992**, *269*, 195.
14. Schermann, C.; Pichou, F.; Landau, M.; Cadez, I.; Hall, R. I. *J. Chem. Phys.* **1994**, *101*, 8152.
15. Weinberg, W. H. In *Dynamics of Gas-Surface Interactions*; Rettner, C. T., Ashfold, M. N. R., Eds.; Royal Society of Chemistry: 1991; pp 171-219.
16. Shin, H. K. *Chem. Phys. Lett.* **1995**, *319*, 235.
17. Shin, H. K. *J. Phys. Chem. A* **1998**, *102*, 2372.
18. Gates, S. M.; Kunz, R. R.; Greenlief, C. M. *Surf. Sci.* **1989**, *207*, 364.
19. Adelman, S. A. *J. Chem. Phys.* **1979**, *71*, 4471.
20. Tully, J. C. *J. Chem. Phys.* **1980**, *73*, 1975.
21. Radeke, M. R.; Carter, E. A. *Phys. Rev. B* **1996**, *54*, 11803.
22. Kim, Y. H.; Ree, J.; Shin, H. K. *J. Chem. Phys.* **1998**, *108*, 9821.
23. Huber, K. P.; Herzberg, G. *Constants of Diatomic Molecules*; Van Nostrand Reinhold: 1979.
24. van de Walle, C. G.; Street, R. A. *Phys. Rev. B* **1995**, *51*, 10615.
25. Kratzer, P.; Hammer, B.; Norskov, J. K. *Phys. Rev. B* **1995**, *51*, 13432.
26. Tully, J. C.; Chabal, Y. J.; Raghavachari, K.; Bowman, J. M.; Lucchese, R. R. *Phys. Rev. B* **1985**, *31*, 1184.
27. Vidali, G.; Ihm, G.; Kim, H.-Y.; Cole, M. W. *Surf. Sci. Rep.* **1991**, *12*, 133.
28. Huheey, J. E.; Keoter, E. A.; Keiter, R. L. *Inorganic Chemistry*; HarperCollins College Publishers: 1993.
29. Koleske, D. D.; Gates, S. M. *J. Chem. Phys.* **1993**, *99*, 8218.
30. McEllistren, M.; Buehler, E. J.; Itchkawitz, B. S.; Boland, J. J. *J. Chem. Phys.* **1998**, *108*, 7384.
31. Ree, J.; Kim, Y. H.; Shin, H. K. *J. Chem. Phys.* **1996**, *104*, 742.
32. Lim, S. H.; Ree, J.; Kim, Y. H. *Bull. Korean Chem. Soc.* **1999**, *20*, 1136.
33. Struve, W. S.; Krenos, J. R.; McFadden, D. L.; Herschbach, D. R. *J. Chem. Phys.* **1975**, *62*, 404.
34. Takamine, Y.; Namiki, A. *J. Chem. Phys.* **1997**, *106*, 8935.
35. Rettner, C. T.; Auerbach, D. J. *J. Chem. Phys.* **1996**, *104*, 2732.
36. Persson, M.; Jackson, B. *J. Chem. Phys.* **1995**, *102*, 1078.
37. Peden, C. H. F.; Goodman, D. W.; Weisel, M. D.; Hoffman, F. M. *Surf. Sci.* **1991**, *253*, 44.